Tuning the Structural, Thermal, and Optical Properties of 7BA+7OBA Liquid Crystal with Dysprosium-Doped Lithium Zinc Phosphate Phosphor Nanoparticles for Advanced Optoelectronic Applications

Reddipalli Trisanjya^{1*}, Ch. Ravi Shankar Kumar² and RKNR Manepalli¹

¹ LCNC Laboratory, Department of Physics, Andhra University, Visakhapatnam-530003, India
²Department of Physics, School of Science, GITAM University, Visakhapatnam-530045, India

*Corresponding Author email: trisanjyareddipalli.rs@andhrauniversity.edu.in

Abstract:

This research investigates the synergistic effects of incorporating dysprosium-doped lithium zinc phosphate (Li₄Zn(PO₄)₂:Dy³⁺) nanoparticles into a binary liquid crystal system composed of p-n-heptylbenzoic acid (7BA) and p-n-heptyl oxybenzoic acid (70BA). By dispersing the phosphor nanoparticles at varying concentrations (1.5 wt%, 2.5 wt%, and 3.5 wt%), the study explores the resulting changes in the structural, thermal, and optical characteristics of the liquid crystal matrix. The Li₄Zn(PO₄)₂:Dy³⁺ nanoparticles were synthesized via a combustion technique and verified through X-ray diffraction (XRD), confirming their successful integration into the LC mixture. Scanning electron microscopy (SEM) alongside energy-dispersive X-ray spectroscopy (EDS) revealed a uniform nanoparticle dispersion, ensuring consistent interaction with the host material. Optical studies using UV-VIS spectroscopy indicated a progressive reduction in the optical bandgap from 4.04 eV to 3.99 eV as nanoparticle concentration increased, highlighting the tunable optoelectronic potential of the system. Differential scanning calorimetry (DSC) and polarized optical microscopy (POM) were employed to track phase transitions and texture evolutions, offering insight into mesophase behavior modifications. Furthermore, FTIR analysis identified subtle spectral shifts in C=O, C=C, and C-H stretching regions, reflective of molecular interactions between the liquid crystals and nanoparticles. Overall, the integration of Li₄Zn(PO₄)₂:Dy³⁺ phosphor nanoparticles into the 7BA+7OBA matrix offers a promising approach to tailoring liquid crystal performance, paving the way for nextgeneration display systems and optoelectronic innovations.

Keywords: Liquid crystalline 7BA,7OBA, Dysprosium, XRD, SEM, FTIR, DSC, POM, Optical

Introduction:

Liquid crystals (LCs) have revolutionized modern technology, emerging as vital materials across a broad spectrum of scientific and industrial fields. They form the technological backbone of highresolution displays, e-readers, and advanced biomedical imaging platforms, including hyperspectral imaging and ophthalmic diagnostics. Their highly adaptable optical properties make them indispensable in precision optical devices such as wave plates, retarders, rotators, and polarization controllers. Beyond these applications, LCs continue to drive advancements in complex optical processing systems, constantly expanding the frontiers of innovation and functionality.[1] Most materials transition directly from a structured crystalline form to a disordered, uniform liquid, certain exceptional substances take a different path entering a remarkable state of matter that blends the order of solids with the fluidity of liquids. These

materials, known as liquid crystals (LCs), form an intermediate phase referred to as the mesophase that exhibits directional order while remaining flowable. Liquid crystals are the driving force behind the vibrant displays in smartphones, laptops, televisions, and countless other digital devices. Beyond screens, their unique optical and electro-mechanical properties unlock a growing frontier of innovation. Recent breakthroughs have spotlighted their pivotal role in shaping next-generation materials, including advanced holographic plastics with tunable lightmanipulating capabilities [2]. Thermotropic liquid crystals have emerged as some of the most technologically significant materials, owing to their remarkable and versatile properties. applications span a wide array of fields, including display technologies, advanced optical devices, biomedical imaging, smart windows, and sensor systems. They also play crucial roles in photonics, cosmetics, lubrication technologies, microwave

Letters in High Energy Physics ISSN: 2632-2714

components, constant current devices, and even in cutting-edge areas like cancer diagnostics [3]. In recent years, nanomaterials have taken center stage as transformative agents propelling the evolution of nanoscience and nanotechnology, unlocking unprecedented possibilities across scientific and technological frontiers. Owing to their nanoscale dimensions, nanomaterials exhibit extraordinary optical, magnetic, electronic, and chemical behaviors traits that have opened new horizons for both groundbreaking research and next-generation industrial technologies. Especially noteworthy are their pronounced electro-optic and thermo-optic responses, driven by high birefringence and significant dielectric anisotropy. These remarkable attributes position nanomaterials as pivotal components in the creation of advanced, highperformance functional materials [4,5]. The deliberate integration of nanoparticles (NPs) into liquid crystal (LC) systems has unlocked exceptional enhancements in their optical and electrical functionalities. Among these, metal nanoparticle-doped LCs stand out for their markedly thermo-optic and improved electro-optic performance. A diverse range of nanoparticles including semiconducting, ferroelectric, metallic, inorganic, carbon-based, and ferro-nematic types has demonstrated significant promise in elevating efficiency electro-optic of LC-based technologies [6,7]. When embedded into nematic LCs, these nanoparticles bring about transformative changes in the material's structural dynamics, altering key features such as morphology, texture, phase behavior, and transition temperatures [8-13]. Phosphate-based materials have emerged as highly attractive hosts for rare-earth ion doping, owing to their environmentally benign composition, cost efficiency. and versatile PO₄ tetrahedral coordination framework. Their widespread adoption in display panel technologies highlights their commercial relevance and practical utility. Notably, when doped with alkali and/or alkaline earth metals, these phosphate hosts exhibit wide bandgaps (Eg) in the ultraviolet region along with moderate phonon energies characteristics that synergistically enhance their luminescence efficiency, making them ideal candidates for high-performance optoelectronic applications[14,15]. Incorporating rare-earth nanoparticles like Dy3+ into liquid crystal systems induces significant modifications in their electrooptical characteristics [16,19]. The evolution toward

solid-state lighting marks a significant leap in replacing traditional lighting systems with solutions that are more energy-efficient, cost-effective, and environmentally sustainable. White light-emitting diodes (LEDs) are central to this transition, yet ongoing advancements are necessary to achieve finely tunable color output and enhanced luminous efficiency. These LEDs typically utilize blue or near-ultraviolet chips in combination with phosphor materials to produce white light [20]. Rare-earthdoped phosphors play a vital role in this technology, offering high emission intensity and narrow spectral bandwidths that make them ideal for a variety of advanced applications. including bioimaging. temperature sensing, optical heating, and therapeutic treatments. Among these, Dy3+ ions are particularly noteworthy due to their ability to emit across multiple wavelengths blue, yellow, and faint red facilitating the generation of high-quality white light. Their strong color purity and potential use in artificial photosynthesis further emphasize their value in sophisticated luminescent systems. However, the efficiency and uniformity of Dy3+ emission are highly dependent on the choice of host matrix, making it a critical factor in the design of next-generation white LED materials [21]. Among standout mesogenic compounds, alkylbenzoic acid and p-n-alkyloxy benzoic acid hereafter grouped as p-n-alkyl(oxy)benzoic acids have garnered significant attention. Their distinct molecular configurations and exceptional intrinsic properties make them ideal building blocks in the design and development of advanced liquid crystal materials. These versatile compounds often serve as crucial intermediates in tailoring functional liquid crystalline systems. [22-24]

This study explores the incorporation of dysprosium-doped phosphor nanoparticles into a liquid crystal matrix composed of *p*-(n-heptyl) benzoic acid (7BA) and *p*-(n-heptyloxy) benzoic acid (7OBA). The nanoparticles were introduced at varying concentrations 1.5 wt%, 2.5 wt%, and 3.5 wt% using a combination of magnetic stirring and ultrasonic bath techniques to ensure uniform dispersion. The primary aim is to assess how the inclusion of Dy³+-activated phosphor nanoparticles influences the structural, electrical, and optical characteristics of the 7BA+7OBA liquid crystal system, with the ultimate goal of advancing

materials for next-generation electro-optic applications.

1.MOLECULAR STRUCTURE

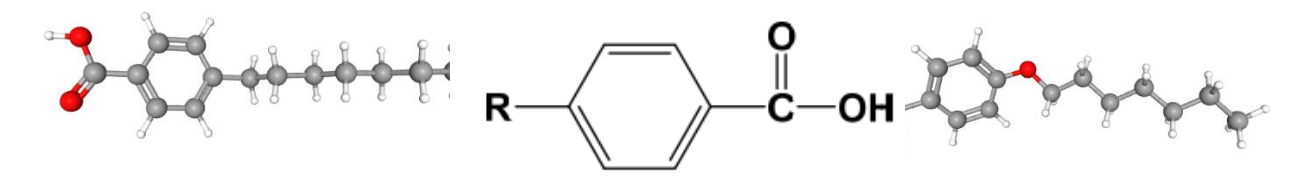
Aromatic acids substituted with alkyl or alkoxy chains are known to exhibit mesomorphic behavior, primarily driven by the formation of hydrogenbonded dimers through their carboxylic acid groups. Among these, p-n-alkyl(oxy)benzoic acid mesogens have become key molecular systems in liquid crystal research. In these structures, p-n-alkylbenzoic acids (7BA) feature alkyl chains directly bonded to the benzene ring, whereas p-n-alkyloxy benzoic acids (70BA) incorporate alkyloxy groups alkyl chains connected via an intervening oxygen atom. The presence of the aromatic core lends both types a generally planar geometry, which is favorable for mesophase formation. However, the mode of substitution direct carbon linkage in 7BA versus ether linkage in 70BA introduces subtle variations in molecular conformation and flexibility. These differences, although minor in structure, can lead to significant changes in the thermal and phase

behavior of the resulting liquid crystalline materials [25].

In alkyloxy benzoic acids, the carboxylic acid group (-COOH) plays a pivotal role in establishing intermolecular hydrogen bonds, particularly through interactions involving the carbonyl (C=O) stretching region. These hydrogen bonds can form either with hydroxyl (-OH) groups of neighboring molecules or with hydrogen atoms on the aromatic ring. What sets alkyloxy benzoic acids (70BA) apart is the presence of ether-linked oxygen atoms within their molecular framework. These oxygen atoms not only enhance intermolecular cohesion between adjacent benzoic acid dimers but also facilitate resonance-assisted hydrogen bonding, making the interactions in (70BA) significantly stronger than those in the alkyl-substituted counterparts (7BA). Moreover, the high electronegativity of the ether oxygen contributes to extended conjugation within the dimeric structures, reinforcing the hydrogen bonding network and promoting more stable and robust mesophases in liquid crystalline arrangements [26].

Fig. 1. Molecular structure of mesogenic alkyl(oxy)-benzoic acids, where $R=OCnH_2n+1$ (alkyloxy), n – indicates the homologue number [i.e, n=7]

 $R = CnH_2n+1$ (alkyl) and



p-n-heptyl benzoic acid (7BA) (C₁₄H₂₀O₂)

2. MATERIALS AND METHODS

2.1 Preparation of 7ba + 7oba mixture:

At first the *p-n*-heptyl benzoic acid (7BA) and *p-n*-heptyloxy benzoic acid (7OBA) acquired from Sigma-Aldrich (St. Louis, MO, USA), was employed without undergoing supplementary purification procedures, were taken in equal amounts i.e., 500 mg each and both were dissolved simultaneously in ethyl alcohol and stirred with magnetic stirrer for about 3h. Then the liquid crystal was placed in ultrasonic bath about 1 h. The resultant

p-n-heptyloxy benzoic acid (7OBA) (C14H20O3)

compound was dried which results the homogenous liquid crystal.

2.2. Synthesis of Dysprosium (Dy³⁺) doped phosphor nanoparticles (DP)

In this study Dysprosium doped lithium zinc phosphate nanoparticles [Li₄Zn (PO₄)₂:Dy³⁺] (DP) were synthesized using the combustion method [27], which offers various benefits over conventional solid-state processes, including reduced processing temperatures and improved phase purity, was used

in this investigation to create DP nanoparticles [Li4Zn (PO4)2:Dy3+]. In an agate mortar, 3.21 g of lithium carbonate, 1.772 g of zinc oxide, and 5.002 g of ammonium phosphate were first finely ground to start the synthesis. To assure homogeneity, 0.373 g of dysprosium oxide (0.1 mole) was added to this homogenized product and further processed. Then, 0.3 g of boric acid (which acted as a flux) and 3 g of urea (which acted as a fuel) were added. After that, the final composite was placed in an autoclave and heated to 800°C for about an hour. This process yielded the desired (DP) nanoparticles composite with refined geometrical characteristics.

2.3 Synthesis of 7BA+7OBA with DLZP-NPs

The resulting product, 7BA+7OBA, was created via a solution-based method and is infused with a number of DP nanoparticles at different concentrations (1.5, 2.5, and 3.5 weight percent). First, a magnetic stirrer was used to dissolve 100 mg of 7BA+7OBA in 5 mL of ethyl alcohol and agitate the mixture at 600 rpm for an hour at 60°C. Following this 1.5 weight percent of DP nanoparticles was added to the solution, the resulting compound was continuously stirred for two to three hours before being exposed to ultrasonic treatment. Following the solvent's evaporation, a 7BA+7OBA-1.5wt% was obtained.

This procedure was methodically carried out again with larger phosphor nanoparticle concentrations of 2.5 weight percent and 3.5 weight percent, producing a liquid crystal nanoparticle matrix. traits employing a variety of sophisticated analytical methods

3. RESULTS AND DISCUSSIONS

3.1: XRD Studies:

To examine the structural properties of Dy3+-doped phosphor nanoparticles synthesized concentration of 2.5 weight percent, powder X-ray diffraction (XRD) analysis was carried out using a Bruker D8-Advance diffractometer (Model No: 216730). The XRD patterns, shown in Fig. 1(a), show distinct diffraction peaks at 2θ values of 10.0° , 11.9°, 17.9°, 21.5°, 23.2°, 24.9°, and 28.7°, which correspond to the (h k l) planes (0 1 1), (1 1 0), (1 3 0), (1 0 2), (1 4 1), (2 2 1) and (2 1 2), respectively, as referenced in the JCPDS database (Card No: 00-720-0940). This confirms the successful incorporation of Dy3+ ions into the phosphor nanoparticles within the 7BA+7OBA matrix. Furthermore, the crystallite size of the Dy3+-doped phosphor nanoparticles was determined using the Debye-Scherrer equation, complemented by Unit Cell software calculations, resulting in an estimated size of 88.92 nm [28].

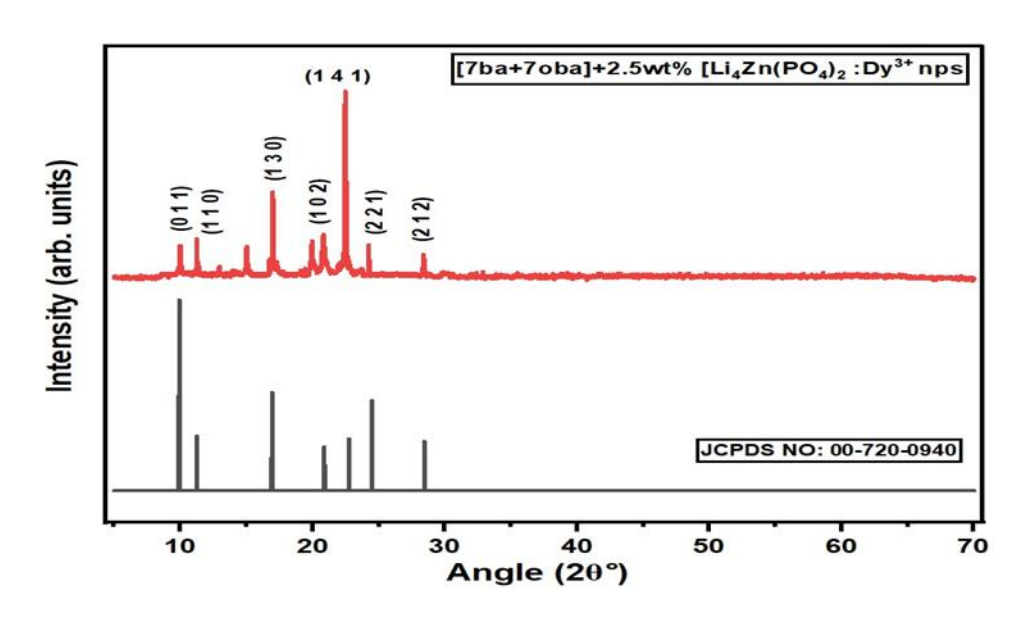


Fig.1(a): XRD Analysis of 7BA+7OBA dispersed in 2.5wt% Li₄Zn(PO₄)₂:Dy³⁺phosphor nps

3.2 SEM Analysis:

Scanning Electron Microscopy (SEM) employed to examine the structural characteristics of liquid crystal nanocomposite Li₄Zn(PO₄)₂:Dy³⁺, with FESEM-TESCAN-MIRA providing valuable insights into the nanoparticle size, morphology, and distribution within the 7BA+7OBA liquid crystal system [29,30]. These structural parameters play a crucial role in determining the electro-optical properties of the material, positioning it as a strong candidate for advanced display technologies. The material's electro-optical characteristics are largely determined by these structural features, making it a promising contender for cutting-edge display technology. The and surface topology architecture of the nanoparticles could be seen in great detail because of SEM's high-resolution imaging capabilities [31].

Energy Dispersive Spectroscopy (EDS) was used to examine the elemental composition and distribution throughout the sample in order to supplement this investigation. Figures 2(a) and 2(b) illustrate SEM images and EDS spectra for Dy³+- doped phosphor nanoparticles (1.5 wt%) dispersed within the 7BA+7OBA medium. The EDS analysis confirmed the presence and weight distribution of key elements, including Zn, P, Dy³+, and O, providing a comprehensive profile of the sample's elemental composition.

The SEM findings clearly demonstrate the uniform dispersion of Dy³+-doped phosphor nanoparticles throughout the 7BA+7OBA matrix, indicating their successful integration. This well-distributed nanoparticle arrangement enhances the overall functional performance of the material, reinforcing its suitability for high-efficiency electro-optical applications.

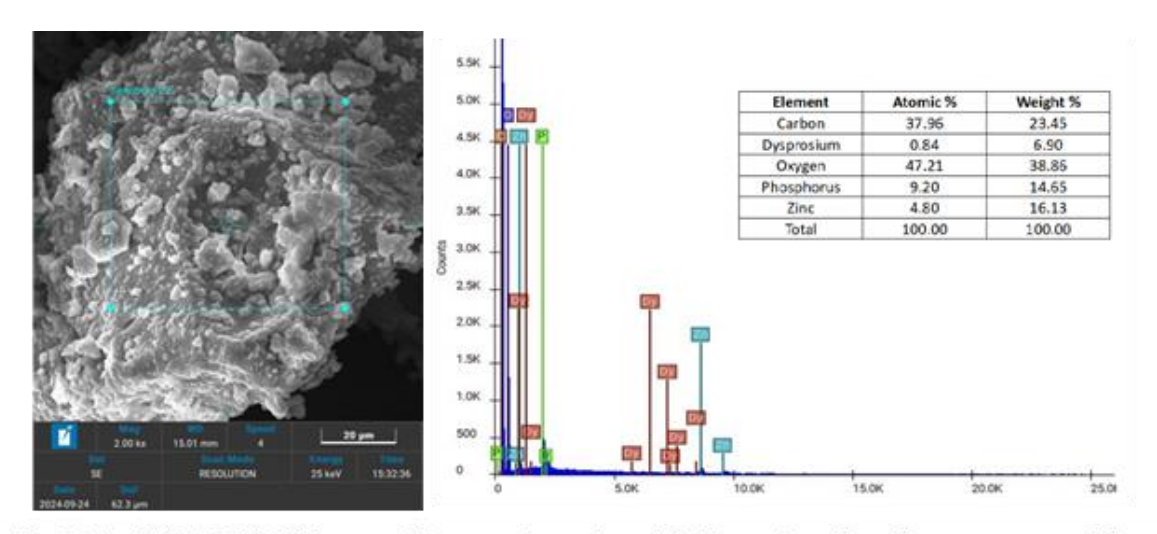


Fig.2(a) SEM & EDS Image of Dysprosium doped lithium zinc phosphate nano particles

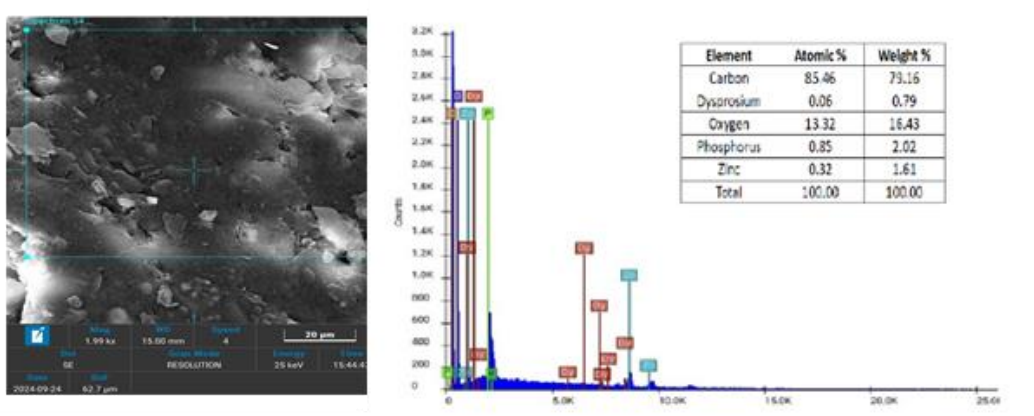


Fig.2(b) SEM & EDS Image of 7BA+7OBA +1.5wt% (DLZ) Dysprosium doped lithium zinc phosphate nano particles

3.3 Ultraviolet-visible spectroscopy:

The absorption behavior of both organic and inorganic materials was examined using UV-visible and spectroscopy, a potent non-destructive analytical method. Using UV-Vis spectrophotometer (Model UV-2450), the optical properties of liquid crystal systems infused with nanoparticles at different concentrations were investigated. Figure 3(a) shows the absorption spectra for the (7BA+7OBA) liquid crystal matrix doped with Dy3+-doped phosphor nanoparticles at concentrations of 1.5 weight percent, 2.5 weight percent, and 3.5 weight percent, throughout the wavelength range of 150-400 nm[32]. The following basic equation describes the relationship between the absorption coefficient (a) and photon energy (hv):

$$\alpha h \nu = A(h \nu - Eg)^n$$

where A is a constant and Eg represents the bandgap energy. The energy bandgap values for the LC system (7BA+7OBA) incorporating different concentrations of Dy³⁺-doped phosphor nanoparticles (Dysprosium-doped lithium zinc phosphate, Li₄Zn(PO₄)₂:Dy³⁺, abbreviated as DLZ) were determined from the plots of photon energy against $(\alpha h \nu)^2$, as depicted in Fig. 3(b).

The UV-Vis analysis revealed that the pristine (7BA+7OBA) exhibited an energy bandgap of 4.04 eV. However, upon the inclusion of Dy³+-doped phosphor nanoparticles, the bandgap exhibited a gradual reduction to 4.03 eV, 4.01 eV, and 3.99 eV for doping concentrations of 1.5 wt%, 2.5 wt%, and 3.5 wt%, respectively. This shift in bandgap values suggests that nanoparticle dispersion significantly influences the electronic state distribution within the host material, consequently altering its optical properties.

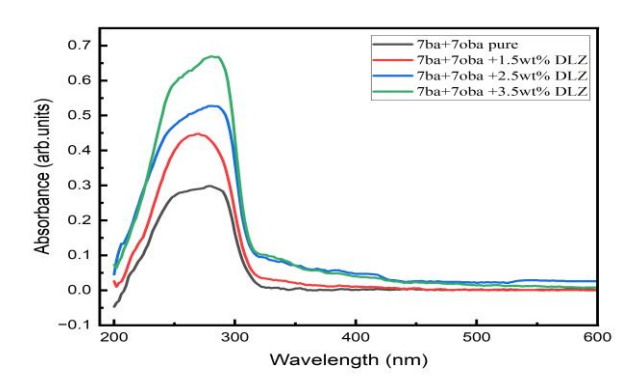


Fig. 3(a) Absorption spectra of 7BA+7OBA Pure & (1.5-3.5 wt%) dispersed Li₄Zn(PO₄)₂:Dy³⁺ phosphor nps

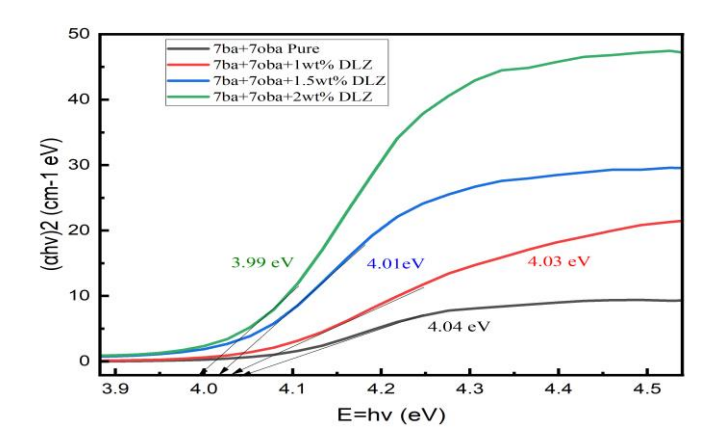


Fig. 3(b) Energy band gap of 7BA+7OBA Pure & (1.5-3.5 wt%) dispersed Li₄Zn(PO₄)₂:Dy³⁺phosphor nps

3.4 Differential scanning calorimetry:

A potent thermal analysis method for measuring heat flow related to phase transitions in materials as a function of temperature and time is differential scanning calorimetry (DSC). Important information on phase transition temperatures and important thermal characteristics, including melting, crystallization, and general thermal stability may be obtained using this technique.

In this study, DSC (Model: STA 7300, Hitachi, Japan) was employed to analyze the thermal behavior of liquid crystal systems doped with nanoparticles at varying concentrations. The phase transition temperatures of pure 7BA+7OBA liquid crystal, as well as those incorporating Dy³⁺-doped phosphor nanoparticles at concentrations of 1.5 wt%, 2.5 wt% and 3.5 wt%, are illustrated in Fig 4(a–c).

The transition temperatures obtained from DSC exhibited strong correlation with those measured using Polarized Optical Microscopy (POM), with minor deviations likely arising from environmental fluctuations. Notably, during the cooling process across the isotropic-nematic (I-N) transition, particularly in the fluctuation-dominated nonlinear region (FDLNR), liquid crystal molecules undergo a loss of rotational symmetry, realigning along a preferred axis known as the director. This molecular reorganization induces abrupt changes in volume and enthalpy, manifesting as heat release during cooling and heat absorption upon heating[33-36]. A comprehensive summary of the recorded phase transition temperatures is provided in Table 1.

Table: 1

S.No	Compound(cooling)	DSC/POM	Transition Temperature (°C)		
			I-N	N-K1	K1-k2
1	Mixture of 7ba + 7oba pure	DSC	132.98	80.94	
		POM	129.5	80.1	78.5
2	Mixture of 7ba+7oba + 1.5wt% Dy ³⁺ doped phosphor nps	DSC	131.99	81.46	
		POM	130.1	84.6	81.4
3	Mixture of 7ba+7oba + 2.5 wt% Dy ³⁺ doped phosphor nps	DSC	132.84	80.71	
		POM	131.9	89.6	79.9
4	Mixture of 7ba+7oba + 3.5 wt% Dy ³⁺ doped phosphor nps	DSC	128.30	79.43	
		POM	127.9	79.2	78.9

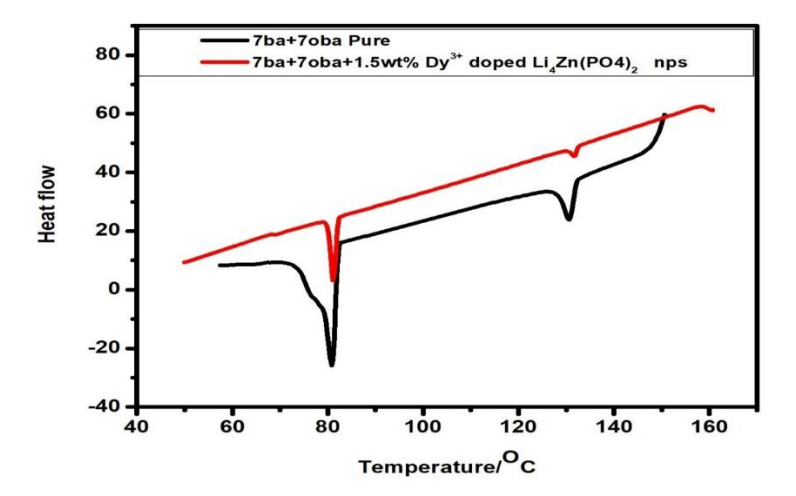


Fig 4(a) DSC Thermograms of Pure 7BA+7OBA with 1.5 wt% Li₄Zn(PO₄)₂:Dy³⁺

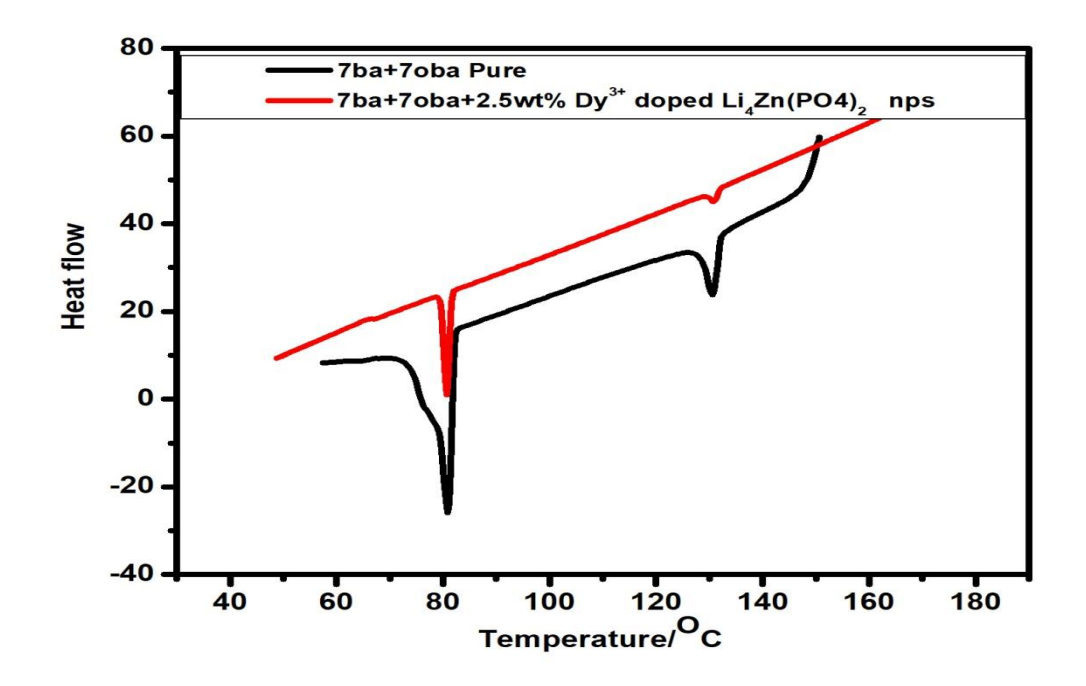


Fig 4(b) DSC Thermograms of Pure 7BA+7OBA with 2.5 wt% Li₄Zn(PO₄)₂:Dy³⁺

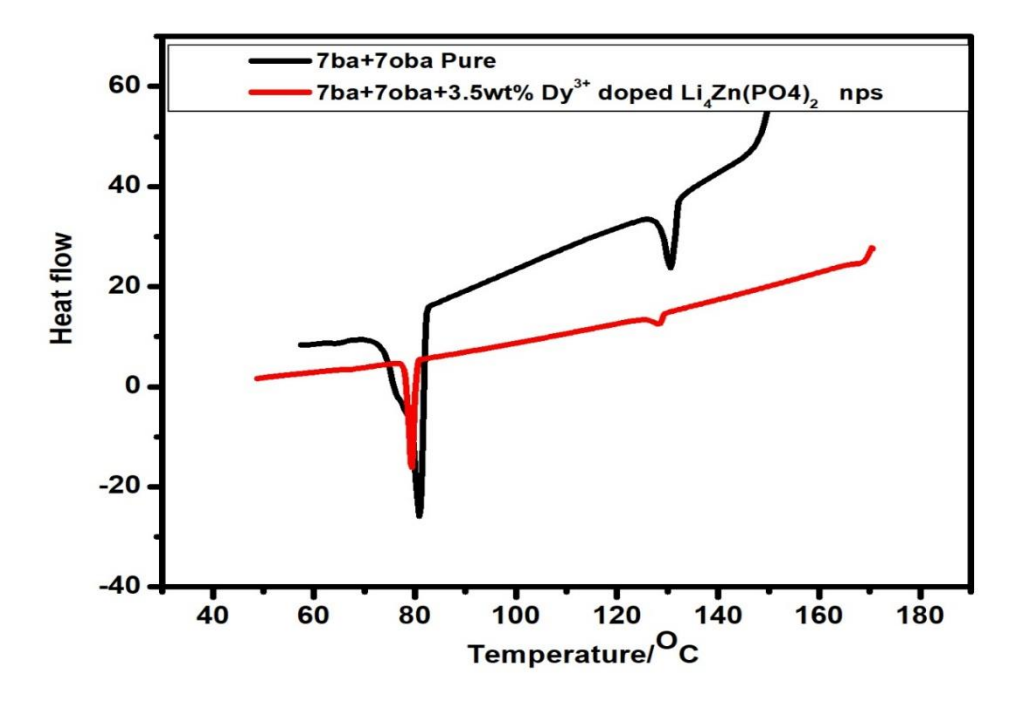


Fig 4(c) DSC Thermograms of Pure 7BA+7OBA with 3.5 wt% Li₄Zn(PO₄)₂:Dy³⁺

3.5 Polarized Optical Microscopy (POM) Analysis

Textural changes linked to phase transitions in a range of liquid crystal (LC) samples were examined using a Polarized Optical Microscope (POM) fitted with a thermal stage. Using a POM (Model: SDTECHS-SDVPM 2727, Manufacturer: SD TECHS), the structural alignment and texture of liquid crystal-nanoparticle composites at varying doping doses were investigated. This analytical method provides vital information on the isotropic and anisotropic properties of LC systems. aiding in the identification of their optical nature as either positive or negative. The POM, operating at 10X magnification, is integrated with a precision-controlled heating block that ensures a temperature accuracy of ± 0.1 °C, regulated through voltage variation. For the experimental procedure, LC mixtures containing varying concentrations of Dy³+-doped phosphor nanoparticles were carefully deposited onto glass slides, covered with slips, and positioned within the heating block as per the methodology described in [37].

Through POM imaging, distinct textures corresponding to the nematic and smectic phases of the LC compounds and their nanocomposites were observed, reflecting changes in molecular orientational order within localized regions. Notably, the nematic phase exhibited characteristic droplet-like and threaded textures, as depicted in Figures 5(a–d) and 5(e–h). While the fundamental LC textures remained largely consistent, a subtle shift in phase transition temperatures was detected, attributed to the influence of nanoparticle dispersion.

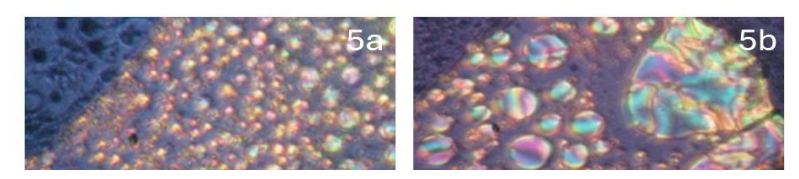


Fig. 5(a-d) POM images of Pure 7ba+7oba (5a) I-N at 129.5°C (5b) Nematic at 120.2°C (5c) Nematic-Solid 80.1°C (5d) Solid 1-Solid 2 at 78.5°C



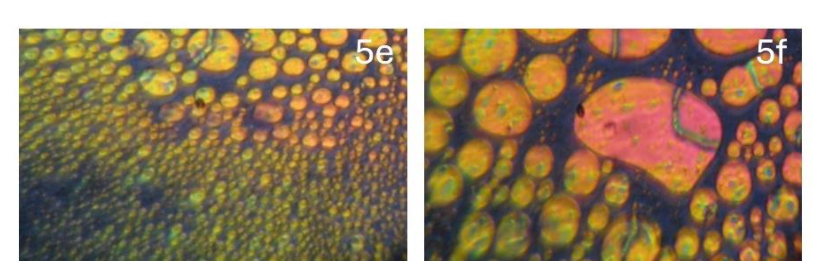


Fig. 5(e-h) POM images of 7ba+7oba+3.5 wt% DLZ (5e) I-N at 127.9°C (5f) Nematic at 119.2°C (5g) Nematic–Solid at 79.2°C (5h) Solid 1-Solid 2 at 78.9°C



3.6 FTIR Studies:

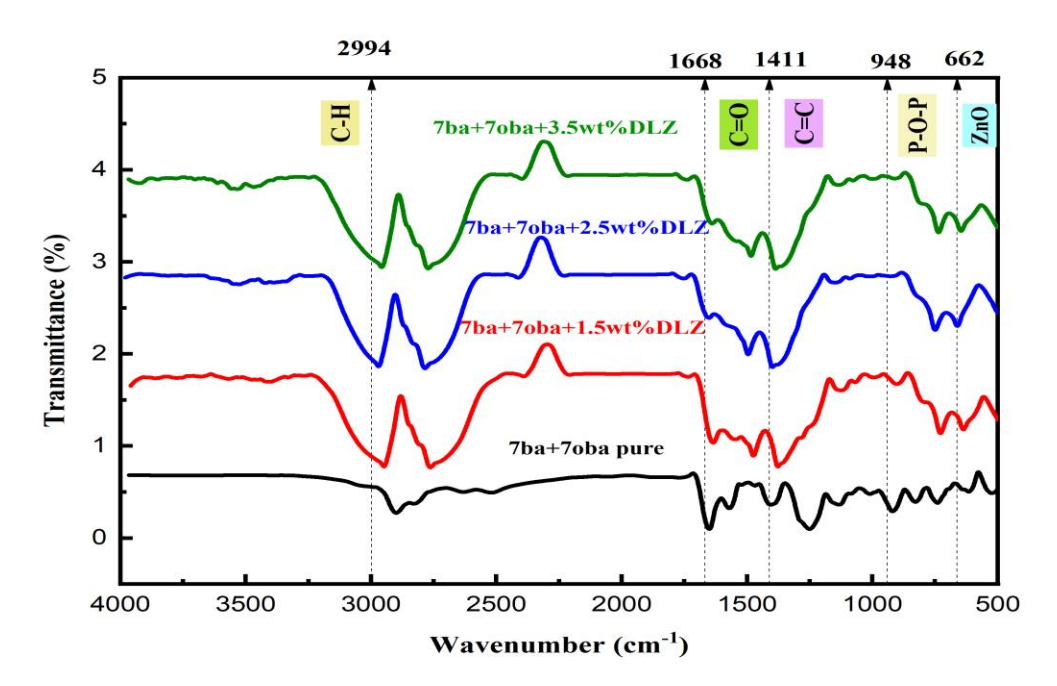


Fig:7 FTIR of 7BA+7OBA Pure & dispersed (1.5-3.5 wt% Li₄Zn(PO₄)₂:Dy³⁺ phosphor nps)

Infrared (IR) spectroscopy serves as a powerful analytical tool for identifying and characterizing organic, inorganic, and polymeric materials by examining their chemical interactions with IR radiation. As molecular vibrations and rotations absorb electromagnetic radiation, unique spectral bands emerge, providing valuable insights into molecular bonding and structural composition.

In this study, Fourier Transform Infrared (FTIR) spectroscopy was employed to investigate the chemical structure of 7BA+7OBA liquid crystal, both in its pure form and when incorporated with Dy3+-doped phosphor nanoparticles at varying concentrations (1.5 wt%, 2.5 wt%, and 3.5 wt%). The spectra, recorded over the 500-4000 cm⁻¹ wavenumber range (Fig. 6), reveal five distinct absorption bands centered around 662 cm⁻¹, 948 cm⁻¹, 1411 cm⁻¹, 1668 cm⁻¹, and 2994 cm⁻¹ [38,39]. The spectral feature at ~662cm⁻¹ corresponds to Zn– O stretching vibrations, while the ~948 cm⁻¹ band is indicative of asymmetric P-O-P linkage stretching [40], confirming the presence of PO₄ tetrahedral structures with well-defined bonding configurations [41,42]. In the mid-to-low frequency region, the spectrum displays a complex interplay of molecular vibrations, including the C=O stretching mode (~1668cm⁻¹) and aromatic ring vibrations [43]. Additionally, the peak at ~1411 cm⁻¹ is attributed to C=C bond stretching [44].

At higher frequencies, strong C–H and O–H stretching vibrations dominate the spectrum. Beneath the intense ν (C–H) peaks (~3000 cm⁻¹), a broad feature corresponding to the Fermi A-type band emerges, linked to the fundamental

O–H stretching vibration (~2994 cm⁻¹) [45,46]. With increasing nanoparticle concentration, notable wavenumber shifts are observed in the C=O, C=C, and

C–H stretching regions, underscoring the dynamic interactions between the liquid crystal matrix and the embedded nanoparticles. Vertical dashed lines in the spectrum serve as reference markers, highlighting the characteristic vibrational signatures of the liquid crystal-nanoparticle composites and providing a comparative framework for structural analysis.

CONCLUSION:

A variety of experimental techniques, such as X-ray diffraction (XRD), scanning electron microscopy (SEM), UV-Vis spectroscopy, differential scanning calorimetry (DSC), polarized optical microscopy (POM), and Fourier-transform infrared (FTIR) spectroscopy, were used to systematically investigate the optical and spectral characteristics of p-(n-heptyl) benzoic acid & p-(n-heptyl oxy) benzoic acid (7BA+7OBA) liquid crystal (LC)

compounds doped with dysprosium-doped lithium zinc phosphate phosphor nanoparticles at varying concentrations (1.5-3.5 wt%). With an estimated crystallite size of 88 nm, XRD measurements verified that the nanoparticles had been successfully incorporated into the LC matrix. The elemental composition and surface morphology were revealed by SEM-EDS analysis, which also verified the existence of phosphorus (P), zinc (Zn), and dysprosium (Dy) in the system. spectroscopy revealed a reduction in optical absorbance upon nanoparticle dispersion, leading to a decrease in the energy gap, indicative of altered electronic properties. Phase transitions were monitored through DSC and POM, which exhibited slight temperature variations, likely due to environmental influences, while maintaining consistency across multiple measurements. FTIR spectroscopy facilitated the identification of functional groups within the LC system, detecting subtle wavenumber shifts, and signifying molecular interactions between the liquid crystal matrix and embedded nanoparticles. The integration of dysprosium-doped lithium zinc phosphate phosphor nanoparticles into the 7BA+7OBA LC system resulted in a notable enhancement of optical, structural, and thermal properties. The presence of nanoparticles modulated absorbance, influenced phase transition behavior, and induced minor shifts in functional group vibrations, making these materials promising candidates for display technologies and optoelectronic applications. Future research will focus on expanding investigations to other liquid crystal systems and exploring their dielectric properties for next-generation electronic devices.

Acknowledgment

The authors thank Advanced Analytical Laboratory, Andhra University, and GITAM University, Visakhapatnam for providing characterization facilities.

Function of the funding sources: There are no funding sources for the study presented in this article.

Conflict of Interest: With relation to the publishing of this article, the authors affirm that they have no conflicts of interest.

References:

- [1] Yuriy Garbovskiy and Iryna Glushchenko, Crystals 5, 501-533; doi:10.3390/cryst 5040501,(2015)
- [2] Keroles B.R.Suong V.H.Paula , ACS Omega,7,21192. DOI: 10.1021/acsomega.2c02084 (2022)
- [3] Tang j., LiZ.,Xie M.,Luo Y.,YuJ.,Chen Z. Photonic Sens. 14 (2).240203(32 p). DOI:10.1007/s13320-024-0707-3(2024)
- [4] Amit Choudhary, Gautam Singh, and Ashok M.Biradar, Nanoscale,6,7743 DOI: 10.1039/c4nr01325e (2014)
- [5] S.T.Wu,Q.T.Zhang, S.Marder,Jpn. J.Appl.Phys.,37,L1254-L1256(1998)
- [6] G.K.Auernhammer, J.B.Zhao, D.Ullrich Vol Hlmer, Eur. Phys. J.E., Phys. J.E., 30,387-394(2009)
- [7] D.Sikharulidze, Appl.Phys.Lett.,86,033507(2005)
- [8] T.Hegmann,H.Qi,B.Kinkead,V.M.Marx,H.Gir gis,P.A.Heiney, Can.J.Met.Mater.Sci.,48,No.1,1-8(2009)
- [9] P.Martinot-Lagarde, G.Durand, J.Phys., 42,269-275(1981).
- [10] .Rahman, W.Lee, J.Phys. D: Appl. Phys., 42,063 001(2009)
- [11] .K.Misra,A.K.Srivastava,J.P.Shukla,R.Manoh ar,Phys.Scr.,78,065602(2008)
- [12] J.P.F.Lagerwall, and G.Scalia, Curr.Appl. Phys.,12, 1387-1412,doi.org/10.1016/j.cap.2012.03.019(2012)
- [13] O.Stamatoiu, J.Mirzaei, and X.Feng, Top Curr.Chem.,318,331-394doi.org/10.1007/128 2011 233(2012)
- [14] M.Gao,K.Li, Y.Yan,.S.Xin,H.Dai, G.Zhu, and C.Wang,J.Mol.Struct,1228,129471, doi.org/10.1016/j.molstruc.129471(2020)
- [15] L.Yu,H.Song,Z.Liu,L.Yang,and S.L.Z.Zheng,J.Phys.Chem.B,109,11450-11455(2005)
- [16] R Carey,P A Gago-Sandoval,D M Newman and B W J Thomas, Measurement Science and Technology,7(4),p505,DOI 10.1088/0957-0233/7/4/006,(1996)
- [17] Volodymyr Tkachenko, Antigone Marino, Giancarlo Abbate, Society for Information Displays, November ,Pages 896-903,http://doi.org/10.1889/JSID18.11,896 (2010)

- [18] V.Tkachenko, A.Marino, F.D'Amore,L.De Stefano, M.Malinconico,M.Rippa,G.Abbate,Eur.Phys.J .E.14,185-192(2004)
- [19] Keisuke ito,Kazuya Goda,Munehiro Kimura, and Tadashi Akahane , Jpn. J. Appl. Phys. 50 01BB02 DOI 10.1143/JJAP.50.01BB02(2011)
- [20] J.P.F. Lagerwall and G. Scalia ,World Scientific Publishing Co. Pte Ltd in Singapore in (2017).
- [21] Gao M., Li K., Yan Y., Xin S., Dai H., Zhu G., and Wang J, *Journal of Molecular Structure* (Volume 1228) in (2021)
- [22] Sariki P., Balireddy V., Gowri Sankara Rao B., and Ratna Raju M, *Brazilian Journal of Physics* in (Volume 52, Page 210). DOI: 10.1007/s13538-022-01212-6,(2022)
- [23] Mouna D., Taoufik S., Ahlem G., Naoufel B.H., Erwann J., and Yves C, *Journal of Molecular Liquids*, (Volume 367, Page 120510)(2022)
- [24] Alhaddad O.A., Abu Al-Ola K.A., Hagar M., Ahmed H.A. Chair Molecules , 25(7), 1510– 1526. DOI: 10.3390/molecules25071510(2020)
- [25] Shoji M., Tanaka F, Macromol, 35, 7460–7472.[22] Rudzki A., Chruściel J, (2002)
- [26] Zalewski S, J. Therm. Anal. Calorim, 148, 10663–10677. DOI:10.1007/s10973-023-12431-7.31-7(2023).
- [27] Navven A, Venkateswarlu M , Srinivas MVVK, Chandan N, Venkateswara Rao K,Chandana G, Ramakrishna Y, Giridhar G , Biointerface Research in Applied chemistry ,14(3):65, https://doi.org/10.33263/BRIAC143.06 (2024).
- [28] J. C. Nie, J. Y. Yang, Y. Piao, H. Li, Y. Sun, Q. M. Xue, C. M. Xiong, R. F. Dou, and Q. Y Tu, Appl. Phys. Lett., 93, No. 17, 173104 (2008).
- [29] B. D. Viezbicke, S. Patel, B. E. Davis, D. P. Birnie, Phys. Status Solidi B, 252, No. 8, 1700–1710 (2015).
- [30] D. Newbury, D. C. Joy, P. Echlin, C. E. Fioriand, and J. I. Goldstein, Plenum Press, New York (1986)
- [31] P.Jayaprada, M. C. Rao, B. T. P. Madhav, and R. K. N. R. Manepalli, DOI :10.1007/s11182-024-03182-5(2024)
- [32] A.Sharma, P. Malik, R. Dhar, and P. Kumar, Bull. Mater. Sci., 42, 206–215 (2019)

- [33] Mustafa Okumuş,Şükrü Özgan,Süleyman Yılmaz, Brazilian Journal of Physics 44(4):326-333, DOI:10.1007/s13538-014-0217-7(2014)
- [34] V.N.Vijayakumar, M.L.N. Madhu Mohan, Solid State Commun. 149, 2090 (2009)
- [35] B.Katranchev, M. Petrov, Bulg. J. Phys. 31, 111 (2004)
- [36] M.Petrov, P. Simova, Liq. Cryst. 7, 203 (1990)
- [37] V.Balasubramanian, V N Vijayakumar, T Vasanthi,Brazilian Journal of Physics, 53:36(2023)
- [38] H.S. Liu, T.S. Chin, S.W. Yung, Mater. Chem. Phys. 50, 1–10 (1997)
- [39] J.O. Byun, B.H. Kim, K.S. Hong, H.J. Jung, S.W. Lee, A.A. Izyneev, J. Non Cryst. Solids, 190, 288–295, (1995)
- [40] M. Shwetha , B. Eraiah, Journal of Non-Crystalline Solids, Volume 555, 1206221 March(2021), https://doi.org/10.1016/j.jnoncrysol.2020.120 622
- [41] Debnath, S.; Saxena, S.K.; Nagabhatla, V. Catal. Commun. 84, 129–133,(2016) https://doi.org/10.1016/j.catcom.2016.06.018
- [42] Lai, Y.M.; Liang, X.F.; Yang, S.Y.; Wang, J.X.; Cao, L.H.; Dai, B. J. Mol. Struct., 992, 84–88, (2011) https://doi.org/10.1016/j.molstruc.2011.02.04 9.
- [43] Johnson SL, Rumon KA.. J Phys Chem.,69(1):74,doi:10.1021/j100885a013,(19 65).
- [44] K. Sankarranarayanan, C. Kavitha, M.L.N. Madhu Mohan PII: Optik Volume 143, Pages 42-58,(2017) DOI: http://dx.doi.org/doi:10.1016/j.ijleo.2017.06.0 47
- [45] Lee JY, Painter PC, Coleman MM. Macromolecules.;21(4):954–960,(1988).doi:10.1021/ ma00182a019
- [46] Kato T, Wilson PG, Fujishima A, et al. Chem Lett. 1990;11:2003–2006. doi:10.1246/ cl.(1990).